HETEROCYCLES, Vol. 98, No. 10, 2019, pp. 1423 - 1435. © 2019The Japan Institute of Heterocyclic Chemistry
Received, 24th September, 2019, Accepted, 15th October, 2019, Published online, 28th October, 2019
DOI: 10.3987/COM-19-14161

ELUCIDATION OF THE CONFORMATIONAL PROPERTIES OF 3-PYRIDINOYL INDOLES AS INTERMEDIATES OF CANNABIMIMETICS

Koji Araki,[a] Hidetsugu Tabata,[a] Kosho Makino,[b] Ryohei Ujiie,[a] Kohei Sezaki,[a] Hiroshi Nakayama,[b] Tetsuta Oshitari,[a] Hideaki Natsugari,[c] and Hideyo Takahashi*[b]

[a]Faculty of Pharma Sciences, Teikyo University, 2-11-1 Kaga, Itabashi-ku, Tokyo 173-8605, Japan. [b]Faculty of Pharmaceutical Sciences, Tokyo University of Science, 2641 Yamazaki, Noda, Chiba 278-8510, Japan. [c]Faculty of Pharmaceutical Sciences, The University of Tokyo, 7-3-1 Hongo, Bunkyo-ku, Tokyo 112-0033, Japan.

Abstract — The conformations of 3-pyridinoyl indoles, which are intermediates of 5-fluoropentyl-3-pyridinoyl indole, were investigated using their X-ray crystal structures. All derivatives existed as s-*trans* conformers. A pseudo-planar conformation was observed in the 2'-yl isomer of 3-pyridinoyl indoles. On the other hand, twisted conformations were observed in 3-pyridinoyl 2-methylindoles. The conformations of these compounds in solution were also investigated using VT-NMR.

INTRODUCTION

Synthetic cannabinoids, which constitute a majority of the illegal drug market, have *N*-alkyl-3-aroylindole as one of the core structures.[1] The ease of the synthetic strategy[2] enabled dramatically increased modifications at the N-1 and C-3 positions. Therefore, hundreds of species of synthetic cannabinoids with frequent displacement of functional groups or substituents were synthesized by clandestine laboratories and distributed illegally. In order to identify a single compound in a series of closely related structural isomers of synthetic cannabinoids, we decided to prepare a compound library of synthetic cannabinoids as authentic preparations, which should be furnished exclusively to official research institutions. In the course of our preparation of the compound library, we planned to synthesize analogues of 1-(5-fluoropentyl)-3-pyridinoyl indole,[3] which were controlled as designated substances under the

Japanese Pharmaceutical Affairs Law in 2013. Hence, the isomers of 3-pyridinoyl indoles (**1**−**3**) with different substitutional sites (at the 2'-, 3'-, and 4'-positions) (Figure 1) were prepared as intermediates of the synthesis. In order to elucidate the conformation of these compounds, we performed X-ray crystallographic analysis and VT-NMR. Here we report the conformational properties of the differentially substituted isomers of 3-pyridinoyl indoles. The weak interaction between the N atom of pyridine and C2-H of the indole/H of 2-Me of 2-methylindole was suggested in the crystal states of **1a**[4] and **1b**, respectively.

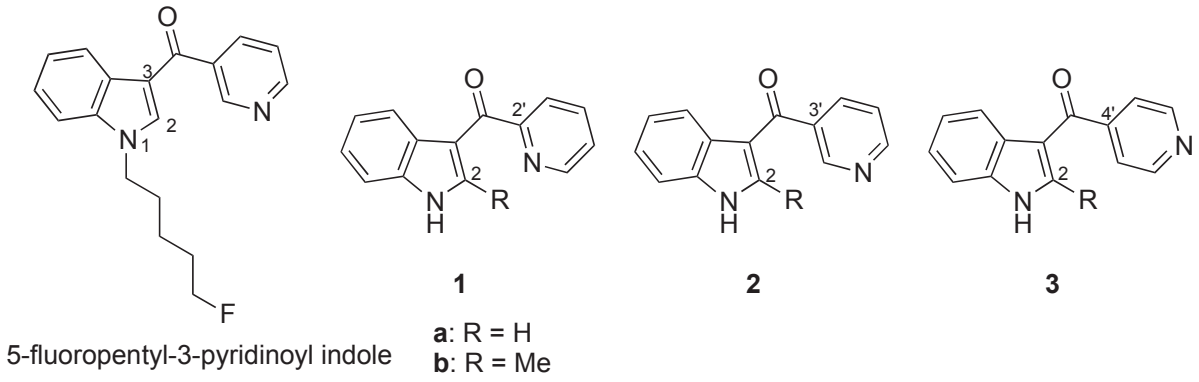

Figure 1. 1-(5-Fluoropentyl)-3-pyridinoyl indole and the isomers of 3-pyridinoyl indoles (**1**−**3**)

RESULTS AND DISCUSSION

1. Preparation

As shown in Scheme 1, the isomers of 3-pyridinoyl indoles (**1**−**3**) were synthesized according to the method reported previously.[5] Friedel-Crafts-type aroylation of indole/5-bromoindole/2-methylindole using 2'/3'/4'-substituted pyridinoyl chloride in the presence of Et_2AlCl provided 3-pyridinoyl indoles **1**−**3**. Because the basic nature of pyridine reduced the reactivity of Lewis acid, the reaction was hampered and gave rather low yields.

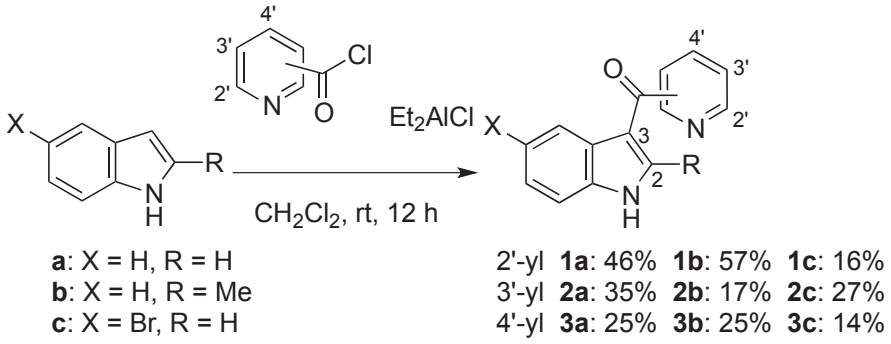

Scheme 1. Preparation of 3-pyridinoyl indoles **1**–**3**

2. Conformational study of 3-pyridinoyl indoles

In the course of the characterization of the synthesized 3-pyridinoyl indoles **1a**, **2a**, and **3a**, we found that the ^{1}H NMR spectrum (in CD_2Cl_2, +23 °C) of 2'-yl isomer **1a** had a characteristic downfield shift of 2-H of indole (at 8.95 ppm). In contrast, the corresponding peak in 3'-yl isomer **2a**[6] and 4'-yl isomer **3a**[7] was observed at 7.72 ppm and 7.71 ppm, respectively. Such a discriminating downfield shift prompted us to conduct a conformational study using X-ray structural analysis. Because of the difficulties in obtaining single crystals of compounds **1a**, **2a**, and **3a**, the more easily crystallized 5-bromo-substituted indole derivatives **1c**, **2c**, and **3c** were subjected to X-ray structural analysis (Figure 2). We believed that the substitution at the outside 5-position of the indole would have little effect on the conformation of the compounds.[8]

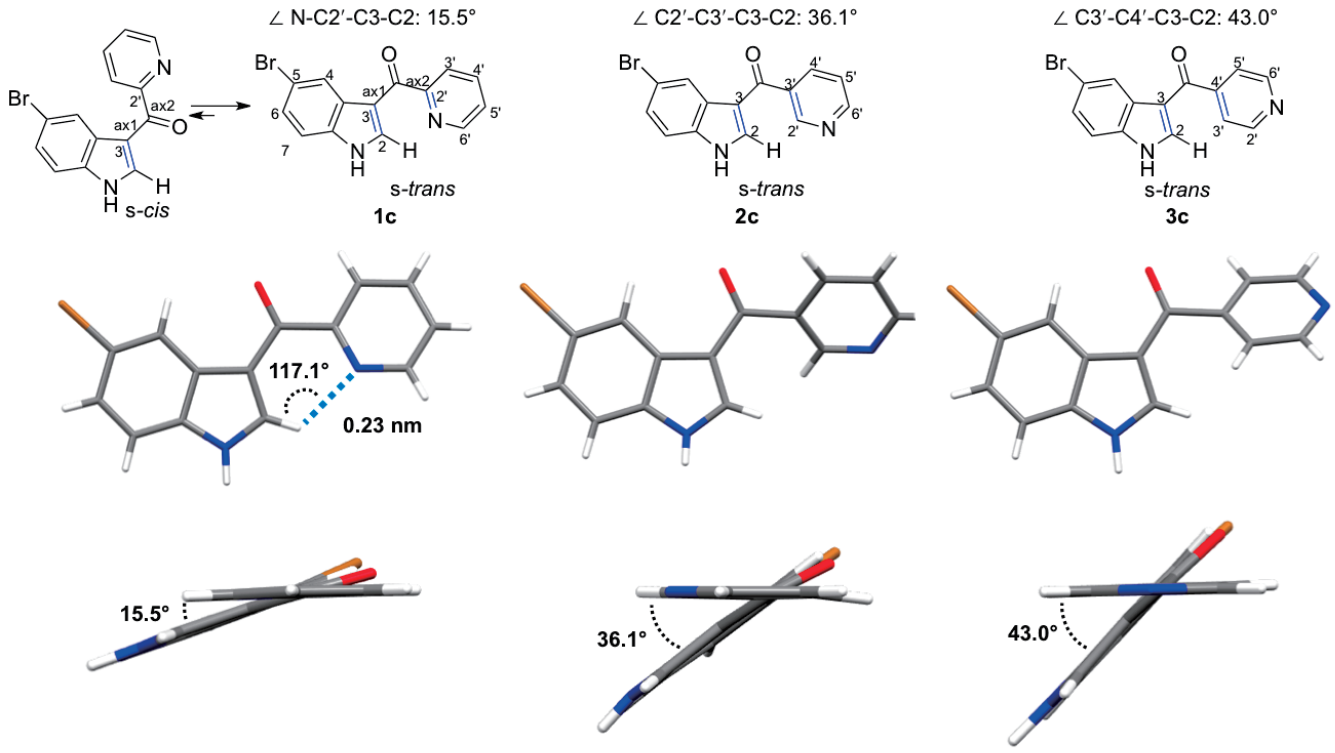

Figure 2. X-Ray crystal structures of **1c**, **2c**, and **3c**

Although two conformers (s-*trans* and s-*cis*) caused by the rotations of the C3–(C=O) axis (ax1) of the ketone moiety were expected,[5] X-ray analysis of **1c**, **2c**, and **3c** confirmed that these compounds exist as s-*trans* conformers (Figure 2). Additionally, 2'-yl isomer **1c** revealed interesting structural features. The twist angle[9] (dihedral angle between the C3–C2 and C2'–N planes) was 15.5°, which was smaller than those of **2c** (36.1°) and **3c** (43.0°), indicating that the pyridine ring and indole ring were arranged in a pseudo-planar conformation. It was also revealed that the distance between 2-H of the indole and

pyridine-nitrogen (C2–H···N) was 0.23 nm and the bond angle (C2–H···N) was 117.1°. According to the criteria for hydrogen bonds,[10] these properties suggest weak bonding.

Since such a pseudo-planar conformation caused by a weak hydrogen bond was observed in the crystal state, we directed our focus to the conformation in the solution state. Thus, the conformations of **1a**, **2a**, and **3a** were examined using VT-NMR (+23 °C ~ +120 °C in DMSO-d_6, −90 °C ~ +23 °C in CD_2Cl_2).[11] In the spectra of 3'-yl isomer **2a** and 4'-yl isomer **3a**, one set of signals remained virtually unchanged (−90 °C ~ +120 °C)[11] (see the Supporting Information). On the other hand, that of **1a** changed characteristically as the temperature was lowered (Figure 3).

(a)

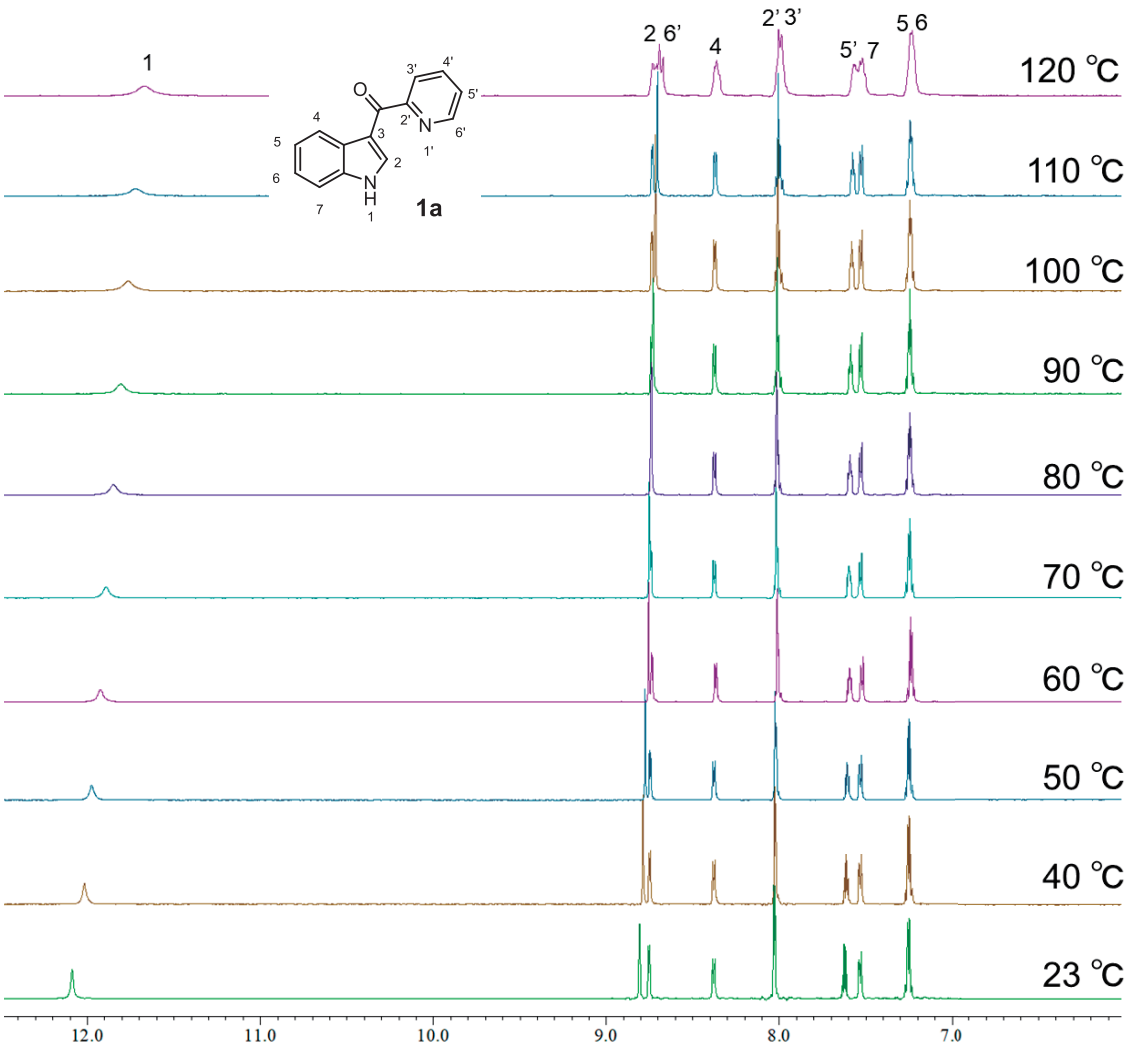

(b)

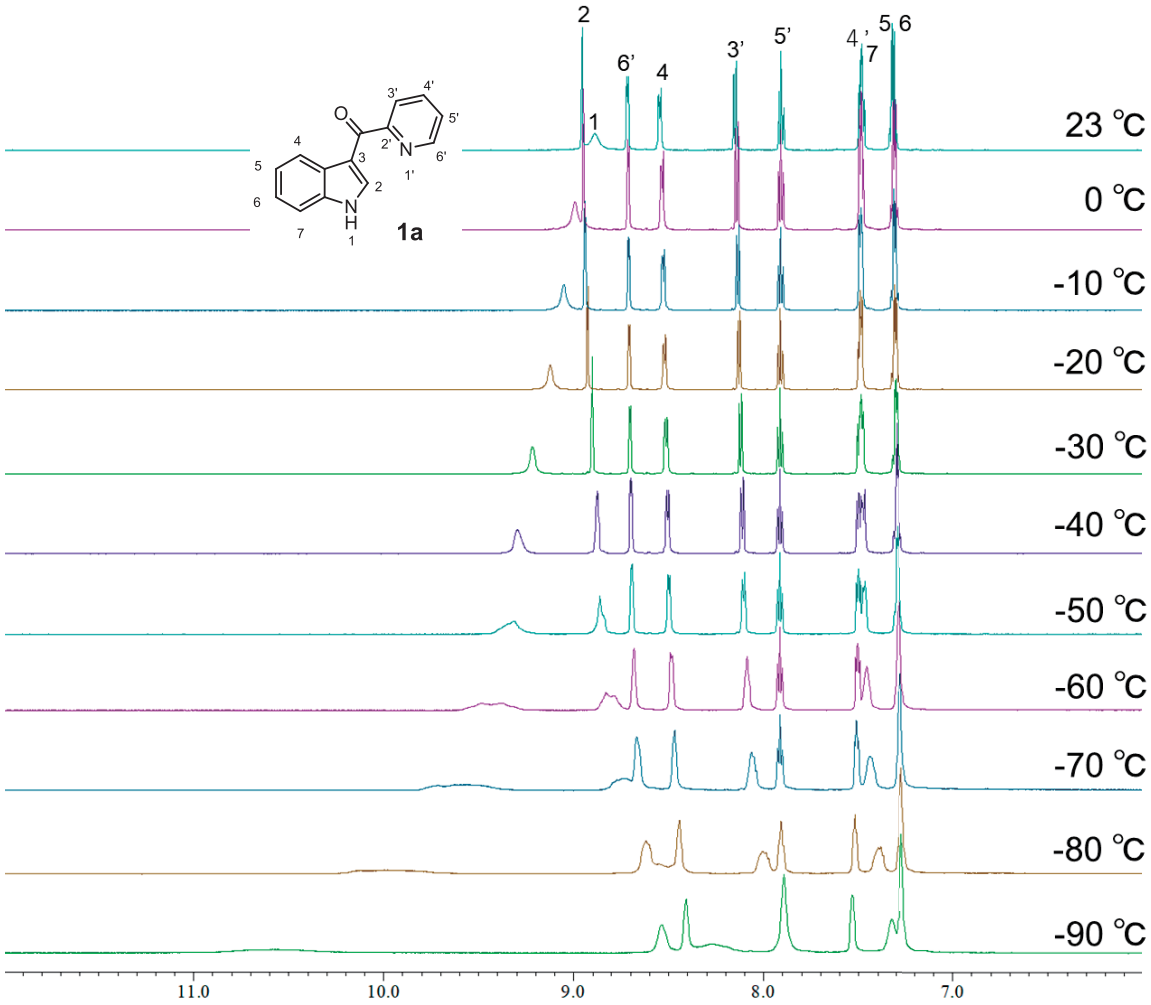

Figure 3. VT-NMR of **1a** (a): +23 °C ~ +120 °C in DMSO-d_6, ; (b): −90 °C ~ +23 °C in CD_2Cl_2

In the VT-NMR spectra of **1a**, one set of sharp signals remained virtually unchanged[12] (−40 °C~ +100 °C), which suggested that the stable s-*trans* conformation observed in the crystal state was maintained. However, the peaks became broad at +120 °C, which might be a sign of the beginning of the conformational change from s-*trans* to s-*cis* caused by the rotation of the C3–(C=O) axis (ax1). In contrast, as the temperature decreased (−40 °C ~ −90 °C), each peak gradually became broad, and the peaks corresponding to 2-H of the indole and 3'-H, 4'-H, and 6'-H of pyridine upshifted. These results indicate that the conformational change around the pyridine moiety caused by the rotation of the (C=O)–C2' axis (ax2) always occurs in solution (−90 °C ~ +120 °C). However, below –40 °C, the rotation of ax2 was partly reduced so that the surrounding hydrogens of pyridine become broad and shifted. Considering that such changes were observed only in 2'-yl isomer **1a**, the electronic interaction between 2-H of the indole and N of pyridine (C2–H···N) somewhat affected the conformation in solution, although the existence of the hydrogen bond was not confirmed.

3. Conformational study of 3-pyridinoyl 2-methylindoles

We conducted further X-ray analysis of 2-methyl-substituted indole derivatives **1b**, **2b**, and **3b** (Figure 4).

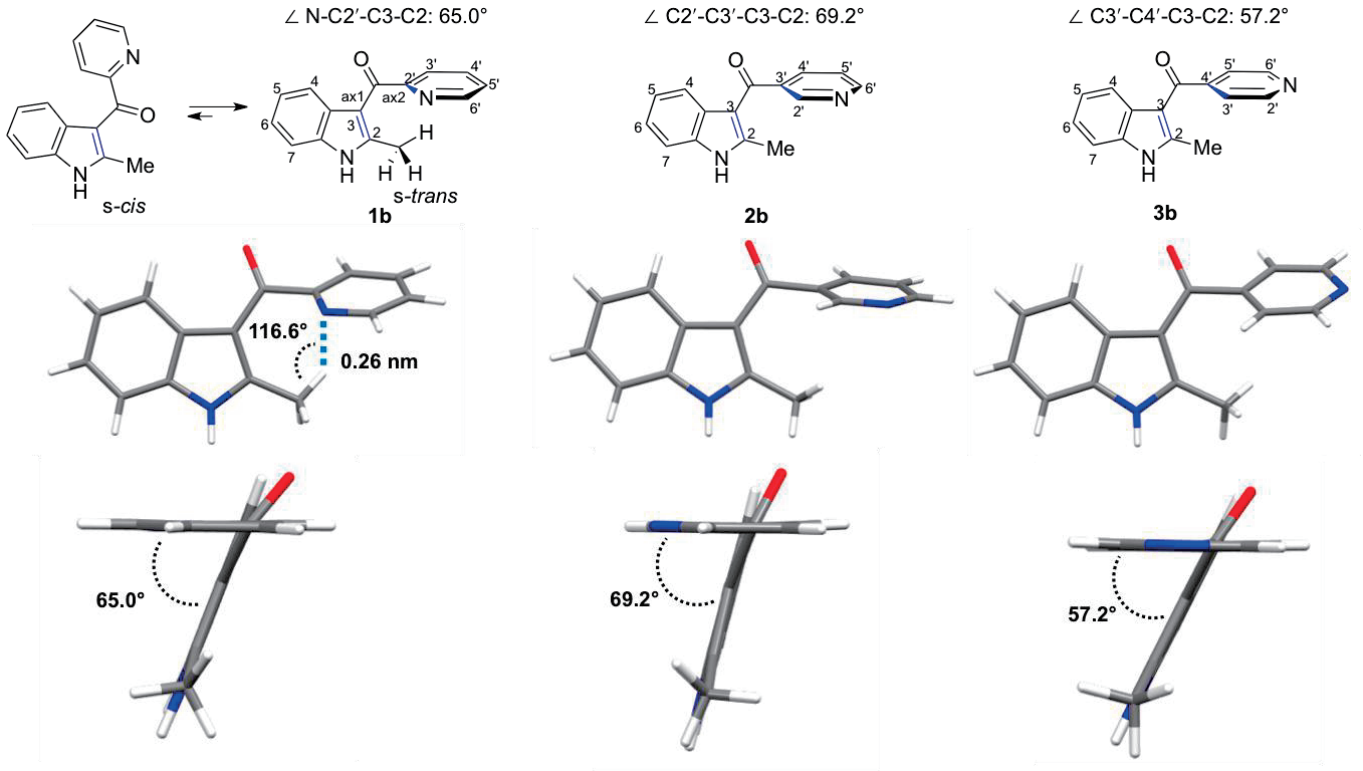

Figure 4. X-Ray crystal structures of **1b**, **2b**, and **3b**

The s-*trans* conformer was similarly observed in each crystal state (Figure 4), although steric hindrance of the 2-methyl substitution caused a more twisted conformation of the indole ring and pyridinoyl moiety. The twist angle (dihedral angle between the C3–C2 and C2'–N planes) in **1b**, **2b**, and **3b** was 65.0°, 69.2°, and 57.2°, respectively. Interestingly, the distance between H of 2-Me of the indole and pyridine-nitrogen (C–H···N) was 0.26 nm and the bond angle (C–H···N) was 116.6° in **1b**, which implied a weak interaction,[10] as shown in Figure 4.

Next, the conformations of **1b**, **2b**, and **3b** in solution were examined using VT-NMR (+23 °C ~ +120 °C in DMSO-d_6; −90 °C ~ +23 °C in CD_2Cl_2).[11]

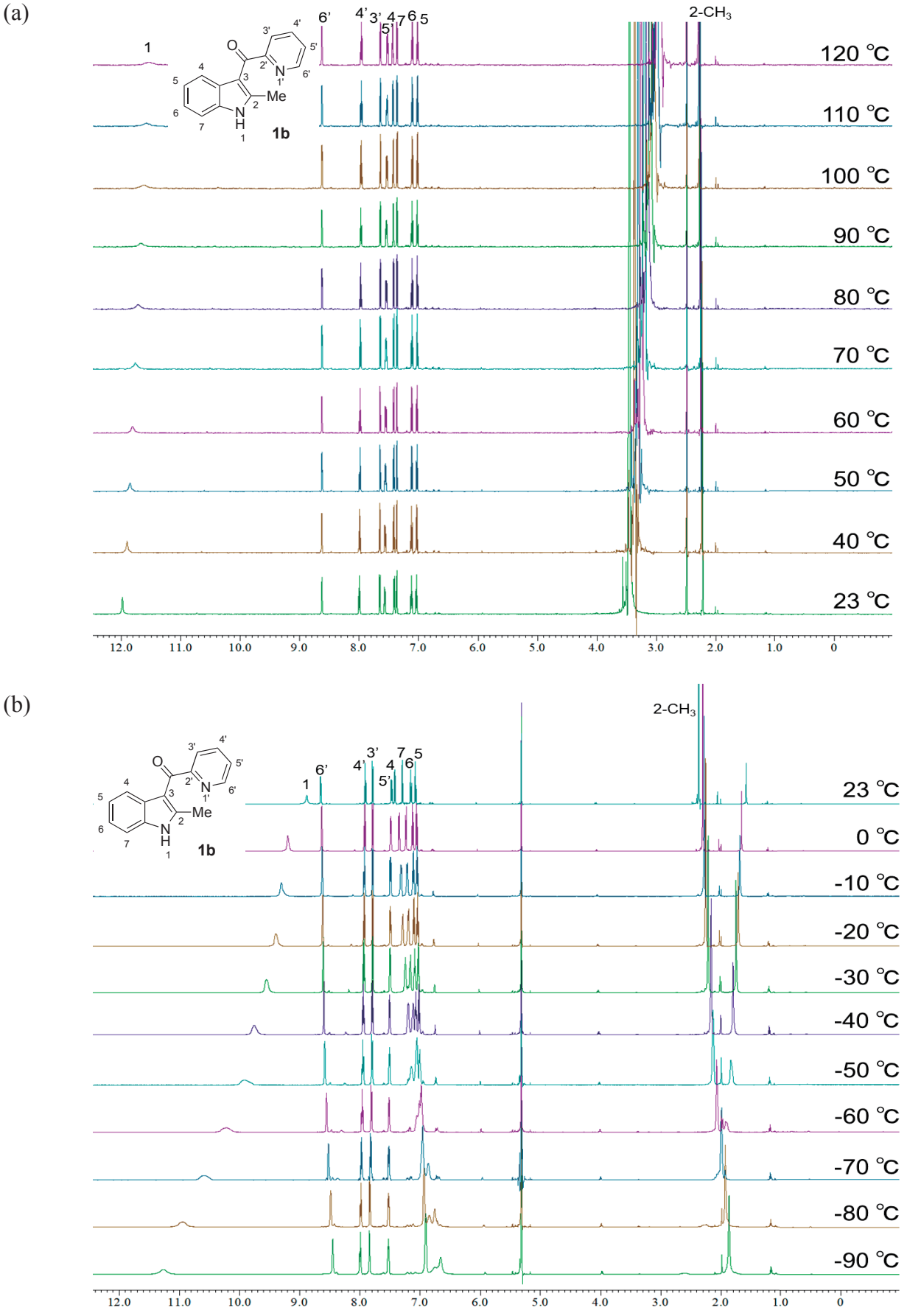

Figure 5. VT-NMR of **1b** (a): +23 °C ~ +120 °C in DMSO-d_6 ; (b): −90 °C ~ +23 °C in CD_2Cl_2

One set of signals remained virtually unchanged[12] (−90 °C ~ +120 °C) in **2b** and **3b**[11] (see the Supporting Information). However, the spectrum of **1b** (Figure 5) at lower temperature was different. As the temperature decreased (−40 °C to −90 °C), peaks corresponding to the indole ring (4-H, 5-H, 6-H, and 7-H) gradually became broader and shifted upfield.[13] At −90 °C, these four peaks were totally fused together at around 6.6−7.0 ppm. In contrast, peaks belonging to pyridine hydrogens (3'-H, 4'-H, 5'-H, and 6'-H) shifted less. Considering these results, the conformational change from s-*trans* to s-*cis* caused by the rotation of the C3–(C=O) axis (ax1) always occur in solution and the averaged spectrum was observed (−40 °C to +120 °C). We assumed that the steric hindrance caused by 2-Me of the indole destabilized the s-*trans* conformation observed in the crystal state, and hence the averaged spectrum of s-*trans* and s-*cis* conformers was observed. As the temperature decreased below −40 °C, the rotation of ax1 may have been reduced so that the surrounding hydrogens of the indole became broad and shifted. Therefore, it appears that the weak interaction between H of 2-Me of the indole and pyridine-nitrogen (C–H···N) observed in the crystal state was not maintained in solution.

4. CONCLUSION

Conformations of 3-pyridinoyl indoles/2-methylindoles **1**−**3** were examined using X-ray crystal structure analysis and VT-NMR. Theoretically, two conformers (s-*trans* and s-*cis*) caused by the rotations of the C3–(C=O) axis (ax1) of the ketone moiety are deduced, although only s-*trans* conformers were observed in all crystal states. In the crystal state of **1c**, the pyridine ring and indole ring were arranged in a pseudo-planar conformation supported by the hydrogen bond between 2-H of the indole and pyridine-nitrogen. In contrast, a twisted conformation in the crystal state was revealed in **1b**, **2b**, and **3b**. In 2'-yl isomer **1b**, a weak interaction between H of 2-Me of the indole and pyridine-nitrogen (C–H···N) was suggested. VT-NMR spectra revealed that the weak interaction existing in the crystal states of **1b** and **1c** were not observed in the solution state. The understanding of weak interaction related to N of pyridine described in this paper may give information on the structure–activity relationships of synthetic cannabinoids.

EXPERIMENTAL

General remarks: All reagents were purchased from commercial suppliers and used as received. Reaction mixtures were stirred magnetically, and the reactions were monitored by thin-layer chromatography (TLC) with precoated silica gel plates. Column chromatography was performed using silica gel (45–60 μm). Extracted solutions were dried over anhydrous $MgSO_4$ or Na_2SO_4. Solvents were

evaporated under reduced pressure. NMR spectra were recorded on a spectrometer at 600 MHz for ^{1}H NMR and 150 MHz for ^{13}C NMR at 296 K unless otherwise stated. Chemical shifts are given in parts per million (ppm) downfield from tetramethylsilane as an internal standard, and coupling constants (*J*) are reported in Hertz (Hz). Splitting patterns are abbreviated as follows: singlet (s), doublet (d), triplet (t), quartet (q), multiplet (m), and broad (br). The high-resolution mass spectra (HRMS) were obtained with an ionization mode of ESI. IR spectra were recorded on an FT-IR spectrometer equipped with ATR (Diamond). Melting points were recorded on a melting point apparatus and are uncorrected.

(2-Methyl-1*H*-indol-3-yl)-2-pyridinylmethanone (1b).

Pale pink solid (yield 57%), mp 196−198 °C: ^{1}H NMR (600 MHz, DMSO-d_6) δ 11.98 (br, 1H), 8.64 (ddd, *J* = 1.2, 1.2, 4.8 Hz, 1H), 8.01 (ddd, *J* = 1.2, 7.2, 7.2 Hz, 1H), 7.67 (dd, *J* = 1.2, 7.2 Hz, 1H), 7.58 (ddd, *J* = 1.2, 4.8, 7.2 Hz, 1H), 7.43 (d, *J* = 8.4 Hz, 1H), 7.38 (d, *J* = 8.4 Hz, 1H), 7.13 (t, *J* = 8.4 Hz, 1H), 7.04 (t, *J* = 8.4 Hz, 1H), 2.24 (s, 3H); ^{13}C NMR (150 MHz, DMSO-d_6) δ 190.3, 158.5, 148.7, 145.7, 137.4, 135.0, 127.5, 125.2, 122.1, 122.0, 121.3, 120.3, 112.2, 111.2, 14.4; IR (ATR) 1535 cm^{-1}; HRMS (ESI-TOF) *m/z*: $[M+H]^+$. Calcd for $C_{15}H_{13}N_2O$ 237.1022; found 237.1023.

(5-Bromo-1*H*-indol-3-yl)-2-pyridinylmethanone (1c).

Pale orange solid (yield 16%), mp 256−257 °C: ^{1}H NMR (600 MHz, DMSO-d_6) δ 12.27 (br, 1H), 8.91 (s, 1H), 8.77 (dd, *J* = 1.8, 4.8 Hz, 1H), 8.53 (d, *J* = 2.4 Hz, 1H), 8.06–8.02 (m, 2H), 7.65 (ddd, *J* = 1.2, 4.8, 7.8 Hz, 1H), 7.52 (d, *J* = 9.0 Hz, 1H), 7.40 (dd, *J* = 2.4, 9.0 Hz, 1H); ^{13}C NMR (150 MHz, DMSO-d_6) δ 186.0, 155.7, 148.6, 139.0, 137.5, 134.9, 128.7, 126.4, 125.6, 123.8, 122.9, 114.9, 114.4, 113.2; IR (ATR) 1566 cm^{-1}; HRMS (ESI-TOF) *m/z*: $[M+H]^+$. Calcd for $C_{14}H_{10}N_2OBr$ 300.9971; found 300.9988.

1*H*-Indol-3-yl-3-pyridinylmethanone (2a).[6]

Pale orange solid (yield 35%).

(2-Methyl-1*H*-indol-3-yl)-3-pyridinylmethanone (2b).

Pale pink solid (yield 17%), mp 199−200 °C: ^{1}H NMR (600 MHz, DMSO-d_6) δ 12.08 (br, 1H), 8.77 (dd, *J* = 1.8, 4.8 Hz, 1H), 8.75 (d, *J* = 1.8 Hz, 1H), 7.98 (ddd, *J* = 1.8, 1.8, 7.8 Hz, 1H), 7.55 (dd, *J* = 4.8, 7.8 Hz, 1H), 7.41 (d, *J* = 7.8 Hz, 1H), 7.35 (d, *J* = 7.8 Hz, 1H) 7.15 (t, *J* = 7.8 Hz, 1H), 7.05 (t, *J* = 7.8 Hz, 1H), 2.39 (s, 3H); ^{13}C NMR (150 MHz, DMSO-d_6) δ 189.5, 151.6, 148.6, 145.3, 137.1, 135.6, 135.0, 127.1, 123.6, 122.1, 121.3, 119.9, 112.4, 111.4, 14.4; IR (ATR) 1564 cm^{-1}; HRMS (ESI-TOF) *m/z*: $[M+H]^+$. Calcd for $C_{15}H_{13}N_2O$ 237.1022; found 237.1029.

(5-Bromo-1*H*-indol-3-yl)-3-pyridinylmethanone (2c).

Pale orange solid (yield 27%), mp 276−277 °C: ^{1}H NMR (600 MHz, DMSO-d_6) δ 12.38 (br, 1H), 8.95 (s, 1H), 8.79 (d, J = 4.8 Hz, 1H), 8.40 (s, 1H), 8.17 (d, J = 7.8 Hz, 1H), 8.12 (s, 1H), 7.58 (dd, J = 4.8, 7.8 Hz, 1H), 7.51 (d, J = 9.0 Hz, 1H), 7.42 (d, J = 9.0 Hz, 1H); ^{13}C NMR (150 MHz, DMSO-d_6) δ 187.9, 151.8, 148.9, 137.6, 135.6, 135.5, 135.5, 127.9, 126.0, 123.7, 123.7, 123.5, 115.0, 114.5; IR (ATR) 1615 cm^{-1}; HRMS (ESI-TOF) *m/z*: [M+H]$^+$. Calcd for $C_{14}H_{10}N_2OBr$ 300.9971; found 300.9976.

1*H*-Indol-3-yl-4-pyridinylmethanone (3a).[7]

Pale brown solid (yield 25%).

(2-Methyl-1*H*-indol-3-yl)-4-pyridinylmethanone (3b).

Pale orange solid (yield 25%), mp 231−233 °C: ^{1}H NMR (600 MHz, DMSO-d_6) δ 12.13 (br 1H), 8.75 (d, J = 4.8 Hz, 2H), 7.50 (d, J = 4.8 Hz, 2H), 7.40 (d, J = 7.8 Hz, 1H), 7.38 (d, J = 7.8 Hz, 1H), 7.15 (d, J = 7.8 Hz, 1H), 7.06 (d, J = 7.8 Hz, 1H), 2.36 (s, 3H); ^{13}C NMR (150 MHz, DMSO-d_6) δ 189.8, 150.3, 150.3, 148.8, 146.0, 135.1, 127.0, 122.3, 121.6, 121.6, 121.5, 120.0, 111.7, 111.5, 14.5; IR (ATR) 1566 cm^{-1}; HRMS (ESI-TOF) *m/z*: [M+H]$^+$. Calcd for $C_{15}H_{13}N_2O$ 237.1022; found 237.1037.

(5-Bromo-1*H*-indol-3-yl)-4-pyridinylmethanone (3c).

Pale orange solid (yield 14%), mp 276−278 °C: ^{1}H NMR (600 MHz, DMSO-d_6) δ 12.41 (br, 1H), 8.78 (d, J = 4.2 Hz, 2H), 8.40 (s, 1H), 8.09 (d, J = 1.2 Hz, 1H), 7.69 (d, J = 4.2 Hz, 2H), 7.52, (d, J = 9.6 Hz, 1H), 7.43 (d, J = 9.6 Hz, 1H); ^{13}C NMR (150 MHz, DMSO-d_6) δ 188.4, 150.2, 150.2, 146.5, 138.1, 135.7, 127.7, 126.1, 123.5, 122.1, 122.1, 115.1, 114.6, 114.0; IR (ATR) 1617 cm^{-1}; HRMS (ESI-TOF) *m/z*: [M+H]$^+$. Calcd for $C_{14}H_{10}N_2OBr$ 300.9971; found 301.0001.

Crystal data of 1b, 1c, 2b, 2c, 3b, and 3c[14]**:** All measurements were made on a Rigaku Raxis Rapid imaging plate area detector with graphite monochromated Cu-Kα radiation. The data were collected at a temperature of –100 °C. The structure was solved by direct method SIR92 and expanded using Fourier techniques. The non-hydrogen atoms were refined anisotropically. All calculations were performed using the Crystal Structure (Crystal Structure 4.0) crystallographic software package or SHELXL97.

Crystal data of 1b (CCDC: 1954418). $C_{15}H_{12}N_2O$, mp 196–198 °C, *M*r = 236.27, Cu Kα (λ = 1.54187 Å), triclinic, $P\bar{1}$, colorless, block 0.200 × 0.100 × 0.050 mm, crystal dimensions a = 7.3793 (3) Å, b = 8.5137 (3) Å, c = 9.7129 (3) Å, α = 80.807°, β = 82.352°, γ = 78.712°, T = 173 K, Z = 2, V =

587.45 (4) Å^3, D_{calc} = 1.336 gcm^{-3}, μCu Kα = 6.838 cm^{-1}, F_{000} = 248.00, GOF = 1.109, R_{int} = 0.0432, R_1 = 0.0502, wR_2 = 0.1215.

Crystal data of 2b (CCDC: 1954419). $C_{15}H_{12}N_2O$, mp 199–200 °C, *M*r = 236.27, Cu Kα (λ =1.54187 Å), triclinic, *P*-1, colorless, block 0.100 × 0.100 × 0.040 mm, crystal dimensions *a* = 7.3314 (4) Å, *b* = 9.0093 (5) Å, *c* = 9.3743 (4) Å, α =78.142°, β = 84.247°, γ = 77.151°, *T* = 173 K, *Z* = 2, *V* = 589.83 (11) Å^3, D_{calc} = 1.330 gcm^{-3}, μCu Kα = 6.811 cm^{-1}, F_{000} = 248.00, GOF = 1.142, R_{int} = 0.1061, R_1 = 0.0869, wR_2 = 0.1744.

Crystal data of 3b (CCDC: 1954420). $C_{15}H_{12}N_2O$, mp 231–233 °C, *M*r = 236.27, Cu Kα (λ = 1.54187 Å), monoclinic, $P2_1/n$, colorless, block 0.200 × 0.150 × 0.100 mm, crystal dimensions *a* = 12.6657 (2) Å, *b* = 7.65408 (14) Å, *c* = 13.2910 (2) Å, α = 90°, β = 111.0288°, γ = 90°, *T* = 173 K, *Z* = 4, *V* = 1202.67 (4) Å^3, D_{calc} = 1.305 gcm^{-3}, μCu Kα = 6.680 cm^{-1}, F_{000} = 496.00, GOF = 1.000, R_{int} = 0.0721, R_1 = 0.0488, wR_2 = 0.0874.

Crystal data of 1c (CCDC: 1954421). $C_{14}H_9OBrN_2O$, mp 256–257 °C, *M*r = 301.14, Cu Kα (λ = 1.54187 Å), monoclinic, *C*2/c, colorless block 0.150 × 0.100 × 0.050 mm, crystal dimensions *a* = 25.2774 (18) Å, *b* = 7.3174 (4) Å, *c* = 13.5233 (9) Å, α = 90°, β = 108.094°, γ = 90°, *T* = 173 K, *Z* = 8, *V* = 2377.6 (3) Å^3, D_{calc} = 1.682 gcm^{-3}, μCu Kα = 46.179 cm^{-1}, F_{000} = 1200.00, GOF = 1.345, R_{int} = 0.1194, R_1 = 0.0886, wR_2 = 0.1647.

Crystal data of 2c (CCDC: 1954422). $C_{14}H_9OBrN_2O$, mp 275–277 °C, *M*r = 301.14, Cu Kα (λ = 1.54187 Å), orthorhombic, *P*bca, colorless block 0.200 × 0.050 × 0.050 mm, crystal dimensions *a* = 12.4555 (2) Å, *b* = 13.2581 (2) Å, *c* = 14.8054 (3) Å, α = 90°, β = 90°, γ = 90°, *T* = 173 K, *Z* = 8, *V* = 2444.91 (8) Å^3, D_{calc} = 1.636 gcm^{-3}, μCu Kα = 44.908 cm^{-1}, F_{000} = 1200.00, GOF = 1.222, R_{int} = 0.0508, R_1 = 0.0397, wR_2 = 0.1195.

Crystal data of 3c (CCDC: 1954423). $C_{14}H_9OBrN_2O$, mp 276–278 °C, *M*r = 301.14, Cu Kα (λ =1.54187 Å), monoclinic, $P2_1/c$, colorless block 0.150 × 0.100 × 0.050 mm, crystal dimensions *a* = 8.8035 (3) Å, *b* = 16.3977 (4) Å, *c* = 8.6968 (3) Å, α = 90°, β = 107.3810°, γ = 90°, *T* = 173 K, *Z* = 4, *V* = 1198.13 (6) Å^3, D_{calc} = 1.669 gcm^{-3}, μCu Kα = 45.820 cm^{-1}, F_{000} = 600.00, GOF = 1.314, R_{int} = 0.0658, R_1 = 0.0582, wR_2 = 0.1681.

ACKNOWLEDGEMENTS

This work was supported in part by Grants-in-Aid for Scientific Research (C) (19K06980) from the Japan Society for the Promotion of Science.

REFERENCES AND NOTES

1. a) B. B. Yao, S. Mukherjee, Y. Fan, T. R. Garrison, A. V. Daza, G. K. Grayson, B. A. Hooker, M. J. Dart, J. P. Sullivan, and M. D. Meyer, *Br. J. Pharmacol.*, 2006, **149**, 145; b) M. M. Ibrahim, H. Deng, A. Zvonok, D. A. Cockayne, J. Kwan, H. P. Mata, T. W. Vanderah, J. Lai, F. Porreca, A. Makriyannis, and T. P. Malan, Jr., *Proc. Natl. Acad. Sci. U. S. A.*, 2003, **100**, 10529; c) J. W. Huffman and L. W. Padgett, *Curr. Med. Chem.*, 2005, **12**, 1395; d) J. W. Huffman, G. Zengin, M. J. Wu, J. Lu, G. Hynd, K. Bushell, A. L. Thompson, S. Bushell, C. Tartal, D. P. Hurst, P. H. Reggio, D. E. Selley, M. P. Cassidy, J. L. Wiley, and B. R. Martin, *Bioorg. Med. Chem.*, 2005, **13**, 89; e) M. Kusano, M. Yamanaka, K. Zaitsu, H. Nakayama, J. Nakajima, T. Moriyasu, H. Tsuchihashi, and A. Ishii, *Forensic Toxicol.*, 2016, **34**, 304.
2. a) C. X. Yang, H. H. Patel, Y.-Y. Ku, R. Shah, and D. Sawick, *Synth. Commun.*, 1997, **27**, 2125; b) M. M. Faul and L. L. Winneroski, *Tetrahedron Lett.*, 1997, **38**, 4749; c) J. Bergman and L. Venemalm, *Tetrahedron*, 1990, **46**, 6061; d) J. Bergman and L. Venemalm, *Tetrahedron Lett.*, 1987, **28**, 3741; e) W. Anthony, *J. Org. Chem.*, 1960, **25**, 2049; f) D. M. Ketcha and G. W. Gribble, *J. Org. Chem.*, 1985, **50**, 5451; g) J. H. Wynne, C. T. Lloyd, S. D. Jensen, S. Boson, and W. M. Stalick, *Synthesis*, 2004, 2277; h) T. Okauchi, M. Itonaga, T. Minami, T. Owa, K. Kitoh, and H. Yoshino, *Org. Lett.*, 2000, **2**, 1485.
3. N. Uchiyama, M. Kawamura, R. K. Hanajiri, and Y. Goda, *Forensic Sci. Int.*, 2013, **227**, 21.
4. B. J. Stokes, S. Liu, and T. G. Driver, *J. Am. Chem. Soc.*, 2011, **133**, 4702.
5. K. Araki, K. Makino, H. Tabata, H. Nakayama, K. Zaitsu, T. Oshitari, H. Natsugari, and H. Takahashi, *Heterocycles*, 2018, **96**, 910.
6. J. H. Wynne, C. T. Lloyd, S. D. Jensen, S. Boson, and W. M. Stalick, *Synthesis*, 2004, 2277.
7. T. S. Jiang and G. W. Wang, *Org. Lett.*, 2013, **15**, 788.
8. The downfield shift of 2-H of the indole (δ = 8.91 ppm) in the ^{1}H NMR spectrum (in DMSO-d_6) was also observed in **1c**, which indicates a similar weak hydrogen bond.
9. P. J. Cox, D. Kechagias, and O. Kelly, *Acta Cryst.*, 2008, **B64**, 206.
10. G. A. Jeffrey, An Introduction to Hydrogen Bonding, Oxford University Press, Inc., New York, 1997.
11. See the Supporting Information for VT-NMR. In 3'-yl isomers **2a** and **2b** and 4'-yl isomers **3a** and **3b**, both ax1 and ax2 always rotated so that the averaged NMR spectra remained the same (–90 °C ~

+120 °C).

12. Exceptionally, NH of the indole was shifted to a lower field as the temperature decreased.
13. Exceptionally, 2-methyl of the indole remained virtually unchanged (−90 °C ~ +120 °C).
14. CCDC 1954418 (**1b**), CCDC 1954419 (**2b**), CCDC 1954420 (**3b**), CCDC 1954421 (**1c**), CCDC 1954422 (**2c**), and CCDC 1954423 (**3c**) contain the supplementary crystallographic data for this paper. These data can be obtained free of charge from The Cambridge Crystallographic Data Centre via www.ccdc.cam.ac.uk/data_request/cif.